A comparison of hydrocarbon indicators derived from AVO analysis

Hong Feng, Brian H. Russell and John C. Bancroft

ABSTRACT

Numerous approaches have been published which derive fluid indicators (often called direct hydrocarbon indicators, or DHI) from AVO equations. The main idea behind these methods is to use the linearized Zoeppritz equations to extract petrophysical parameters such as P-impedance, S-impedance, bulk modulus, shear modulus, Lamé's parameters, Poisson's ratio, etc. and, from cross-plots of these parameters, infer the fluid content. Often, these indicators provide a good tool to quickly identify hydrocarbon zones. But the question of whether there is a best approach and, if so, which one it is, is still under debate. The purpose of this study is to examine which indicator can most easily discriminate a gas/oil sand from its background geology, and which indicator is most sensitive to pore-fluid content estimation.

INTRODUCTION

The fluid factor (ΔF) was proposed by Smith and Gidlow (1987), and was derived by combining the linearized AVO equation with the mudrock line (Castagna et al., 1985). The authors also combined density and P-wave velocity changes by using Gardner's equation (Gardner et al., 1974). A version of the fluid factor which utilized density was introduced by Fatti et al. (1994). Goodway et al. (1997) suggested that Lamé's elastic parameters λ and μ and their products with density could be useful tools in AVO analysis. Gray et al. (1999) showed how to estimate the parameters $\rho\mu$ and $\rho\lambda$ more directly by a new parameterization of the linearized AVO equation, as does Chen (1999). Russell et al. (2003) introduced the attribute $Ip^2 - cIs^2$ with c being a function of local $(Vp/Vs)^2$, where Vp and Vs are the dry rock P-wave and S-wave velocities.

In this study we used Gassmann fluid substitution to model changes in these parameters at given reservoir conditions in order to analyze the sensitivity of each fluid hydrocarbon indicator. We also examined the numerical example of the class 1, 2, and 3 sand models given by Hilterman (2001) to further examine the performance of these indicators.

METHODOLOGY

The standard approach to AVO analysis is well known and was derived by Shuey (1985) based on the Aki-Richards (Aki and Richards, 1980) linearized formulation of the Zoeppritz equations. Their equation can be written as

$$R_P(\theta) = A + B\sin^2(\theta) + C\sin^2(\theta)\tan^2(\theta), \qquad (1)$$

where A is the normal incident P-wave reflection coefficient Rp(0), B is the AVO gradient, and C is a curvature term that is often considered negligible. The product of A

and B is often used to verify classical bright spots. This is based on the observation that low impedance gas sands encased in shale will have larger negative AVO intercepts (A) and a larger negative AVO gradient (B) than those not associated with gas. Thus A*B should be an excellent indicator of a class III type gas sand. Furthermore, as shown by Swan (1993), product indicators have excellent S/N characteristics and may exhibit some degree of immunity to mild phase and velocity errors. On the other hand, A*B will very effectively screen out Rutherford Class I (positive A, negative B) and Class II (A near-zero, negative B) gas sands. It can also be shown that, if Vp/Vs = 2, the scaled sum A+B gives an estimate of $\Delta\sigma$, the Poisson reflectivity where σ is Poisson's ratio, and the scaled difference A-B gives an estimate of Rs(0), the zero offset shear-wave reflectivity.

The fluid factor as modified by Fatti et al. (1994) is defined by the equation $\Delta F = Rp - g(t)Rs$, where the terms Rp and Rs represent the P and S-wave normal incident reflectivites. The term g(t) represents a time varying scale factor given by the average ratio Vp/Vs multiplied by the linear coefficient in the mudrock line (Castagna et al., 1985). For wet reservoirs, $\Delta F = 0$, and for gas filled reservoirs it will be nonzero. It has been noted that the Fluid Factor and Poisson reflectivity are equivalent when Vp/Vs=2. Lithologies that do not follow the Vp and Vs relationship for brine saturated clastics may produce a fluid factor anomaly. For example, coal produces an anomaly similar to gas sand reservoir. Since carbonates do not follow the criteria for clastic rocks, a carbonate equivalent to the "mudrock line" should be used for carbonate reservoirs.

Elastic constants are fundamental in seismology because the P and S-wave velocities depend on the elastic constants and density of the rock. Thus, the extraction of these elastic constants can help us to understand the rock behavior when the pore fluid changes.

Goodway et al. (1997) proposed the LMR (lambda-mu-rho) method, where L, M, and R represent: λ, the first Lamé parameter; μ the shear modulus or coefficient of rigidity; and ρ, the density. Note also that $\lambda = K - (2/3)\mu$, where K is the bulk modulus. It was observed by Goodway (2001) that various combinations of λ, μ, and ρ, such as, $\lambda\rho$, $\mu\rho$, and λ/μ, show a better separation of gas sand from brine sands and shales than Ip and Is where Ip is P-impedance and Is is S-impedance. An effective fluid indicator can be found on a cross-plot of $\mu\rho = Is^2$ versus $\lambda\rho = Ip^2 - 2Is^2$. The intuitive interpretation of this is that $\lambda\rho$ and $\mu\rho$ are fundamentally more orthogonal than Ip and Is, stemming from the ambiguity in the Vp and Vs velocity relationships that share the same value rigidity μ. Goodway (2001) also argued that the value of λ/μ is a more sensitive indicator than λ, $\lambda\rho$, Vp/Vs, or σ, since the formulation $\lambda/\mu = 2\sigma/(1-2\sigma)$ shows that for a given change in Poisson ratio we see an enhanced change in the λ/μ value.

Batzle et al. (2001) proposed the fluid indicator K-μ. It provides a direct look at the effect of pore fluid on the bulk modulus, and as such is quite similar to $\lambda\rho$ and to the Gassmann fluid indicator described by Hilterman. This indicator works best in a sandstone regime where the clay content may vary from negligible to significant. This method comes from the observation that the bulk modulus for gas saturated or dry clastics is approximately equal to the shear modulus, which is consistent with the laboratory data of Han (1986).

Russell et al. (2003) proposed a method based on Biot-Gassmann theory to extract the fluid term $\rho f = Ip^2 - cIs^2$ from P-wave and S-wave impedances, where Ip and Is are the P-wave and S-wave impedance respectively, ρ is density, and f represents the fluid term. The term c is the local $(Vp/Vs)^2$, Vp and Vs are the P- and S-velocities for dry rock condition. The ρf term is also equivalent to the $\rho \Delta K$ term in Batzle et al. (2001), where ΔK corresponds to the change in saturated bulk modulus due to fluid effects. As discussed by Russell et al., the Goodway (1997) formulation is a particular case of the $Ip^2 - cIs^2$ attribute, where c=2 implies that the dry rock Poisson's ratio is 0. The fluid indicator K-μ proposed by Batzle et al. (2001) is also a particular case of $Ip^2 - cIs^2$ attributes, corresponding to $K_{dry} = \mu$ and c=2.333.

SENSITIVITY ANALYSIS FOR FLUID INDICATORS

Analysis using Gassmann fluid substitution equation

To analyze the sensitivity of each fluid indicator, we used the Gassmann fluid substitution equation (Gassmann, 1951) to model the changes of these parameters at given reservoir conditions. First, the bulk modulus (Ksat) and shear modulus (μ) at in-situ conditions can be estimated from the wire line log data by the equations,

$$K = \rho \left(Vp^2 - \frac{4}{3} Vs^2 \right), \text{ and} \tag{2}$$

$$\mu = \rho Vs^2, \tag{3}$$

where, Vp and Vs are the P-wave and S-wave velocity, K and μ are the bulk and shear moduli, and ρ is the mass density. Using Gassmann fluid substitution, the bulk modulus for dry rock can be derived by the equation

$$Kd = \frac{Ksat \left(\dfrac{\phi Km}{Kf} + 1 - \phi \right) - Km}{\left[\dfrac{\phi Km}{Kf} + \dfrac{Ksat}{Km} - 1 - \phi \right]}, \tag{4}$$

where, Ksat, Kd, Km, Kf are the bulk moduli of the saturated rock, dry rock, mineral matrix, and pore fluid, respectively, and ϕ is porosity. Then, with known Kd, we can estimate Vp and Vs when the pore fluid changes. Finally, various hydrocarbon indicators can be estimated.

We examined the effect of fluid properties on the fluid indicators. The initial state is Vp=11000ft/s, Vs=6500ft/s and ρ=2.2 g/cm3. Figures 1 and 2 show the results for each indicator calculated from the Gassmann fluid substitution equation, including λ, μ, σ, k-μ, $Ip^2 - cIs^2$, Rp-gRs and λ/μ. From Figure 1 and Figure 2, we notice that $Ip^2 - cIs^2$ is the term most sensitive to the fluid change, followed by K-μ and λ.

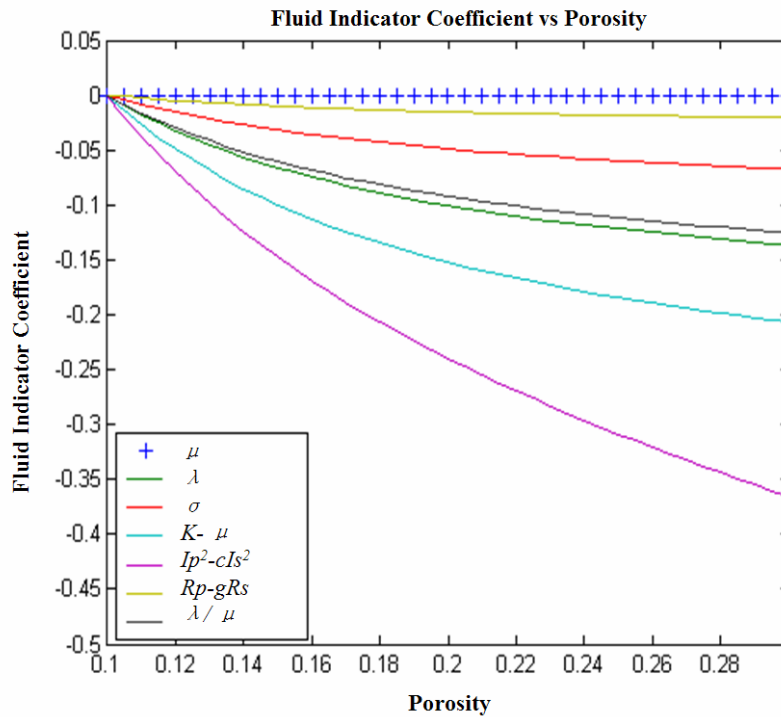**Fluid Indicator Coefficient vs Porosity**

FIG. 1. Fluid indicator coefficients versus porosity. These indicators are calculated using the Gassmann fluid substitution equation with the initial state: Vp=11000ft/s, Vs=6500ft/s, Sw=0.2, ρ=2.2 g/cm3. From these curves, the indicator Ip^2-cIs^2 is most sensitive to the porosity change.

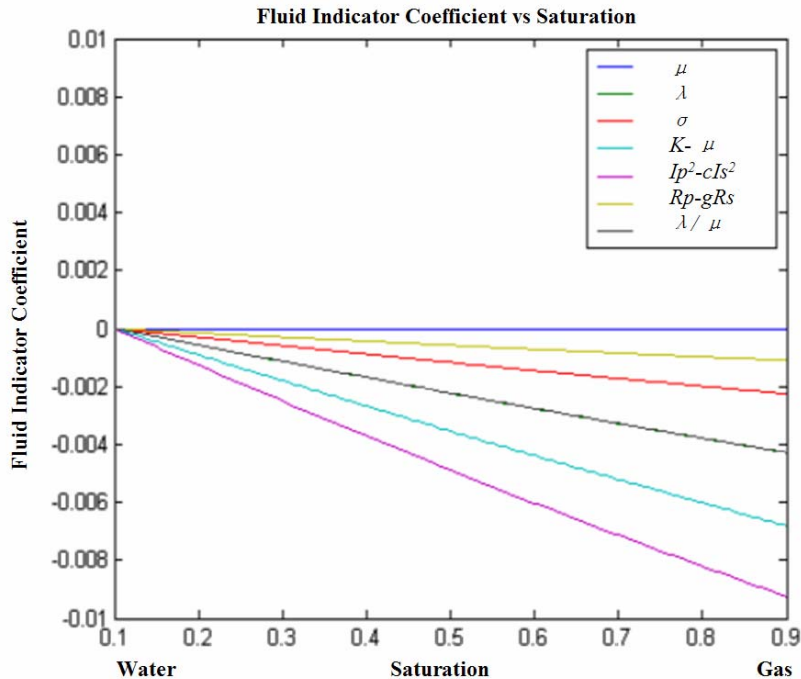**Fluid Indicator Coefficient vs Saturation**

FIG. 2. Fluid indicator coefficients versus saturation. These indicators are calculated using the Gassmann fluid substitution equation with the initial state: Vp=11000ft/s, Vs=6500ft/s, Porosity=0.2 and ρ=2.2 g/cm3. From these curves, the indicator Ip^2-cIs^2 is most sensitive to the saturation change.

Analysis using numerical example

To diagnose the sensitivity of each indicator, let us examine the class I, II, and III sand models given by Hilterman (2001). These models were derived from Gulf of Mexico data. The following twelve indicators: $\Delta\alpha/\alpha$, $\Delta\beta/\beta$, $\Delta\rho/\rho$, ΔK, $\Delta\mu$, $\Delta\lambda$, ΔY, $\Delta\sigma/\sigma$, Δ (Vp/Vs)/(Vp/Vs), K-μ, Ip^2-cIs^2 and ΔF, were chosen for discrimination. The c term in the Ip^2-cIs^2 fluid indicator was chosen to be 2.85. Each fluid indicator coefficient diagnoses the sensitivity to fluid discrimination and is defined as the difference between shale and wet sand or shale and gas sand divided by the value related to the shale reference. From Figures 3 through 5 we can observe that the indicators Ip^2-cIs^2, ΔK, K-μ and $\Delta\lambda$ are more effective than other indicators. Also, there is good separation between wet sand and gas sand for Class I. However, for Class 2 and Class 3 sands, the values decrease and the difference between wet and gas sand decrease, making it very difficult to separate gas sand from wet sand.
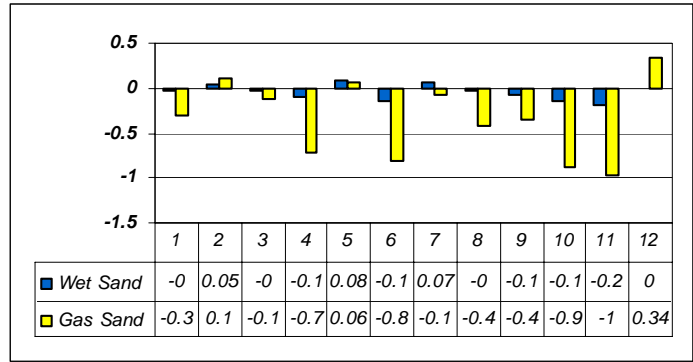
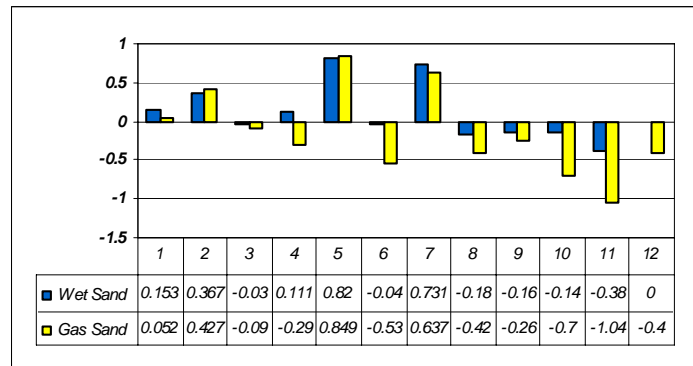|	1	2	3	4	5	6	7	8	9	10	11	12
■ Wet Sand	-0	0.05	-0	-0.1	0.08	-0.1	0.07	-0	-0.1	-0.1	-0.2	0
□ Gas Sand	-0.3	0.1	-0.1	-0.7	0.06	-0.8	-0.1	-0.4	-0.4	-0.9	-1	0.34

FIG. 3. Calculated indicators for Class 1 sand model (4000-ft depth). 1. $\Delta\alpha/\alpha$ 2. $\Delta\beta/\beta$ 3. $\Delta\rho/\rho$ 4. ΔK 5. $\Delta\mu$ 6.$\Delta\lambda$ 7. ΔY 8. $\Delta\sigma/\sigma$ 9. Δ (Vp/Vs)/ (Vp/Vs) 10. K-μ 11. Ip^2-cIs^2,12.ΔF. Observe that the indicators Ip^2-cIs^2, ΔK, K-μ and $\Delta\lambda$ are more effective than other indicators. Also, there is good separation between wet sand and gas sand.

	1	2	3	4	5	6	7	8	9	10	11	12
■ Wet Sand	0.153	0.367	-0.03	0.111	0.82	-0.04	0.731	-0.18	-0.16	-0.14	-0.38	0
□ Gas Sand	0.052	0.427	-0.09	-0.29	0.849	-0.53	0.637	-0.42	-0.26	-0.7	-1.04	-0.4

FIG. 4. Calculated indicators for Class 2 sand model (9000-ft depth). 1. $\Delta\alpha/\alpha$ 2. $\Delta\beta/\beta$ 3. $\Delta\rho/\rho$ 4. ΔK 5. $\Delta\mu$ 6.$\Delta\lambda$ 7. ΔY 8. $\Delta\sigma/\sigma$ 9. Δ (Vp/Vs)/ (Vp/Vs) 10. K-μ 11. Ip^2-cIs^2,12. ΔF. Notice that absolute values of Ip^2-cIs^2, ΔK and $\Delta\lambda$ are still more effective than other indicators. However, their values decrease compared with the class 1 sand model, and the difference between wet sand and gas sand decreases.
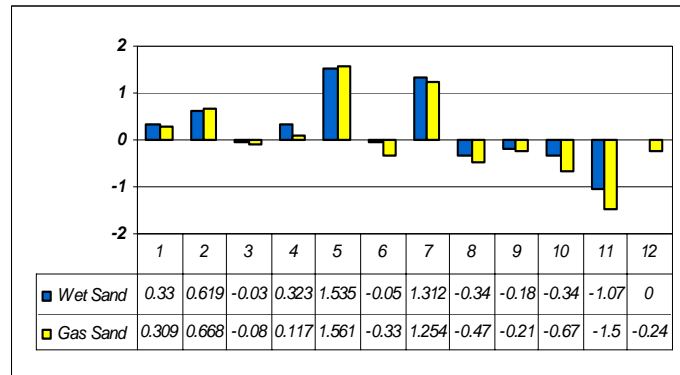
	1	2	3	4	5	6	7	8	9	10	11	12
■ *Wet Sand*	0.33	0.619	-0.03	0.323	1.535	-0.05	1.312	-0.34	-0.18	-0.34	-1.07	0
□ *Gas Sand*	0.309	0.668	-0.08	0.117	1.561	-0.33	1.254	-0.47	-0.21	-0.67	-1.5	-0.24

FIG. 5. Calculated indicators for Class 3 sand model (14000-ft depth). 1. $\Delta\alpha/\alpha$ 2. $\Delta\beta/\beta$ 3. $\Delta\rho/\rho$ 4. ΔK 5. $\Delta\mu$ 6. $\Delta\lambda$ 7. ΔY 8. $\Delta\sigma/\sigma$ 9. $\Delta (Vp/Vs)/ (Vp/Vs)$ 10. K-μ 11. Ip^2-cIs^2 12. ΔF. Notice that the values of Ip^2-cIs^2, ΔK and $\Delta\lambda$ become less compared with class 1 and class 2 sand models. It is not easy to separate wet sand from gas sand just from these indicators, except for $\Delta\lambda$ and ΔF.

Analysis using Castagna and Smith's examples

Castagna and Smith (1994) presented a set of 25 worldwide measurements of P- and S-wave velocities and densities in associated shales, brine-saturated sands and gas-saturated sand. It is instructive to examine this data set in the cross-plot domain. The generated fluid indicators include Ip, Is, λ, μ, σ, k-μ, and Ip^2-cIs^2. Crossplot analysis was conducted to see their discrimination ability between gas-saturated sand, brine-saturated sand and shale.

From the crossplot of $\mu\rho$ versus Ip (Figure 6), there are bad separations in both directions between shale, gas sand and wet sand. However, there is good separation in the K-u direction and bad separation in the Ip direction between shale, gas sand and wet sand (Figure 7). For the crossplot of $\lambda\rho$ versus $\mu\rho$ (Figure 8), there is good separation in the $\lambda\rho$ direction and bad separation in the $\mu\rho$ direction between shale, gas sand and wet sand. Also, from Figure 9, there is overlap in the ρs direction. However, there is a good separation in the ρf direction between shale, gas sand and wet sand. From the crossplot analysis it can be observed that it is easy to discriminate gas sand from wet sand or shale, but it is hard to separate the wet sand from shale.
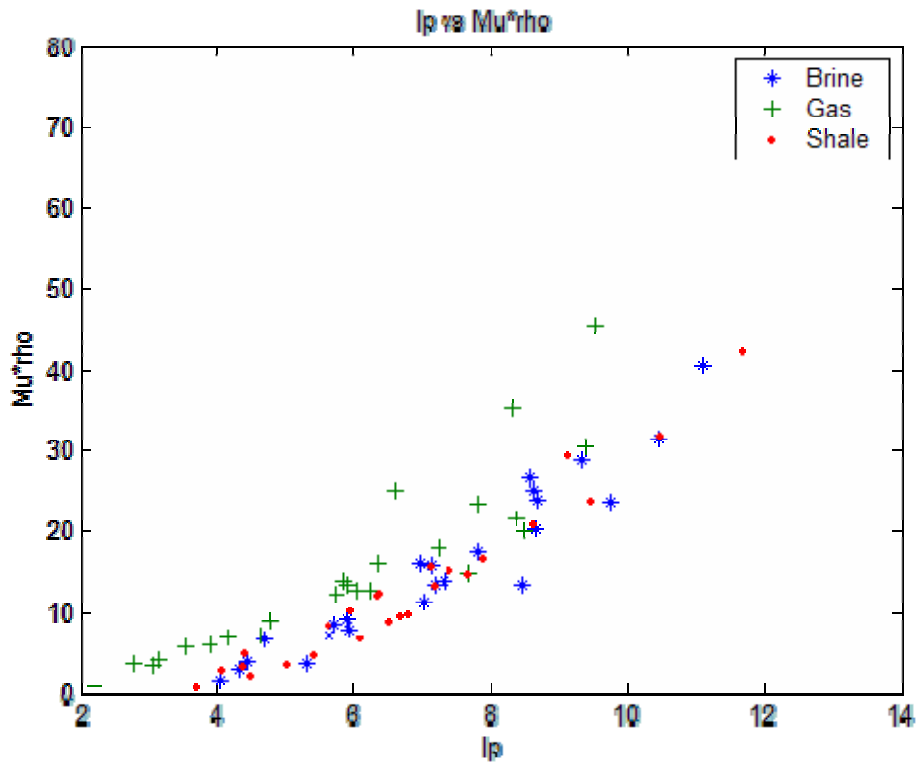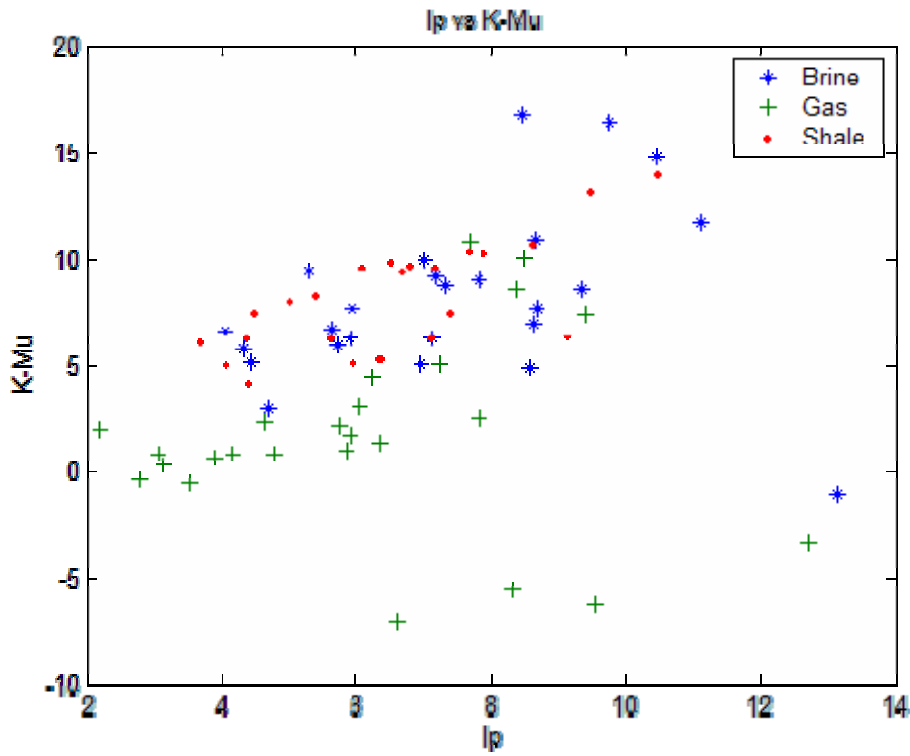
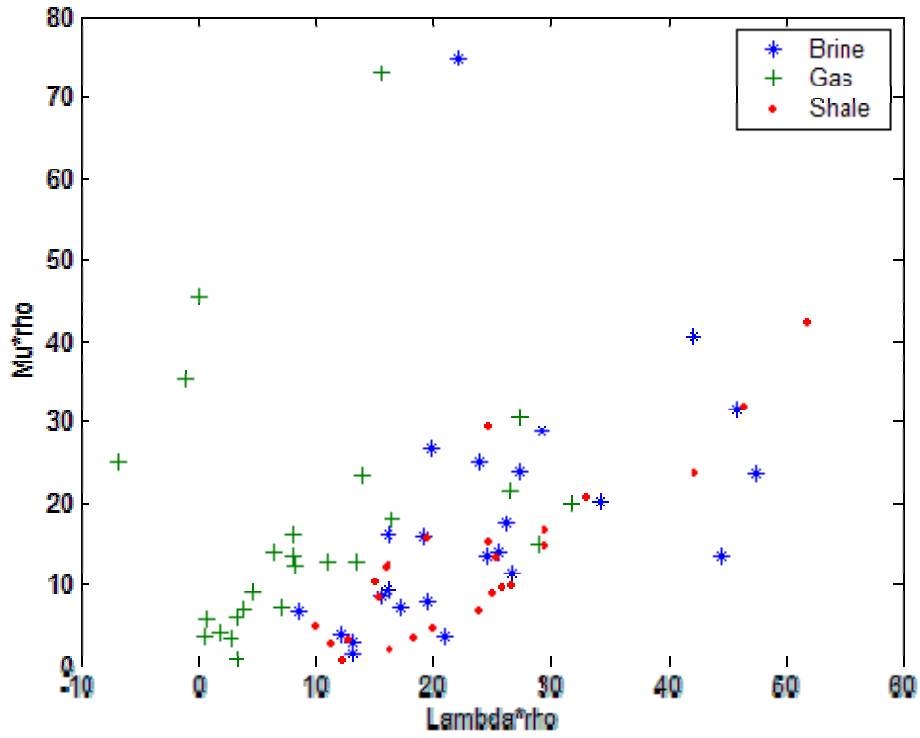FIG. 6 Crossplot of Ip versus μρ

FIG. 7 Crossplot of K-u versus Ip
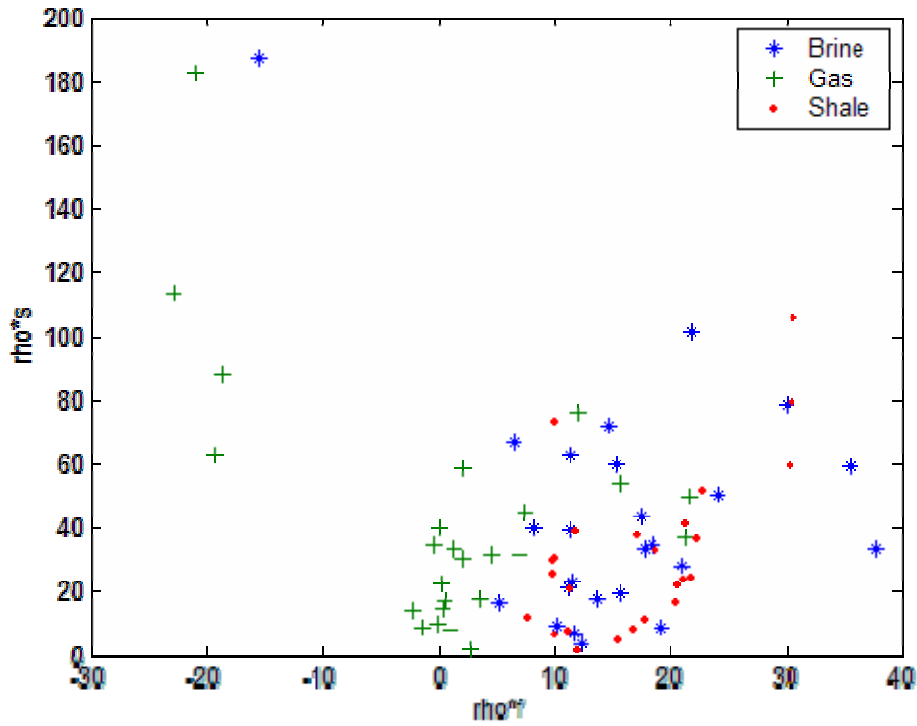
FIG. 8 Crossplot of λρ versus μρ

FIG. 9 Crossplot of ρf versus ρs

CONCLUSIONS

Various combinations of rock properties have been proposed as hydrocarbon indicators and it can be concluded that there is a great deal of equivalence between fluid indicators Ip^2-cIs^2, K-μ, $\lambda\rho$, λ/μ. For sandstones, the difference Ip^2-cIs^2 may be the most sensitive in absolute terms. However, most of these indicators give similar results in magnitude, and each can give insight into the meaning of the other. The best indicator needs to be calibrated and tested for the local situation.

ACKNOWLEDGEMENTS

REFERENCES

Aki, K., and Richards, P.G., 1980, Quantitative seismology: Theory and methods: W. H. Freeman and Co.

Batzle, M., R. Hafmann, D. Han, J. Castangna, Fluids and frequency dependent seismic velocities of rocks: 2001, The Leading Edge, February, p168-171.

Brian H. Russell, Ken Hedlin, Fred J. Hilterman, and Lawrence R. Lines, 2003, Fluid-property discrimination with AVO: A Biot-Gassmann perspective: Geophysics, **68**, 29-39.

Castagna, J. P., Batzle, M. L., and Eastwood, R. L., 1985, Relationship between compressionaland shear-wave velocities in clastic silicate rocks: Geophysics, **50**, 571-581.

Castagna, J. P., Batzle,M. L., and Eastwood, R. L., 1985, Relationships between compressional-wave and shear-wave velocities in clastic silicate rocks: Geophysics, **50**, 571–581.

Chen, X. C., 1999, Essentials of Geomodulus Method, 1999 SEG Expanded Abstracts.

De-Hua, H., and M. Batzle, 2002, Fizz water and low gas-saturated reservoirs: The Leading Edge, **21**, 395–398.

Fatti, J. L., Vail, P. J., Smith, G. C., Strauss, P. J. and Levitt, P. R., 1994, Detection of gas in sandstone reservoirs using AVO analysis: A 3-D seismic case history using the geostack technique: Geophysics, **59**, 1362-1376.

Gardner, G. H. F., Gardner, L. W., and Gregory, A. R., 1974, Formation velocity and density – the diagnostic basis for stratigraphic traps: Geophysics, **39**, 770-780.

Gassmann,F., 1951, Uber die Elastizitat poroser Medien:Vierteljahrsschrift der Naturforschenden Gesellschaft in Zurich, **96**, 1–23.

Goodway W. 2001. AVO and Lame' constants for rock parameterization and fluid detection. Recorder, **26**, 39-60.

Goodway, W., Chen, T., and Downton, J., 1997, Improved AVO fluid detection and lithology discrimination using Lamé petrophysical Parameters; "Lambda-Rho", "Mu-Rho", & "Lambda/Mu fluid stack", from P and S inversions.

Gray, D., Goodway, W. and Chen, T, 1999, Bridging the gap: Using AVO to detect changes in fundamental elastic constants: 1999 SEG meeting abstracts, 852-855.

Han, D., A. Nur, Effects of Porosity and Clay Content on Wave Velocity of Sandstones, Geophysics, **51**, 2093-2107, 1986, Geophysics Reprint 10, 1988.

Hedlin, K., 2000, Pore space modulus and extraction using AVO: 70th Ann. Internat. Mtg., Soc. Expl. Geophys., Expanded Abstracts, 170-173.

Hilterman, F. J., 2001, Seismic amplitude interpretation: Short Soc. Expl. Geophys. Distinguished Instructor Series 4.

Shuey, R.T., 1985. A simplification of the Zoeppritz equations: Geophysics, **50**, p. 609-614.

Smith, G. C. and Gidlow, P. M., 1987, weighted stacking for rock property estimation and detection of gas: Geophys. Prosp., **35**, no. 09, 993-1014.

Swan, H. W., 1993, Properties of direct AVO hydrocarbon indicators in Castagna, J. P., and Backus, M. M., Eds., Offset dependent reflectivity--Theory and practice of AVO analysis: Society of Exploration Geophysics, 78-92.